The Volume Spectral and Energy Efficiency of Ultra-Dense IoT Networks with Clustered Users

Hao Fu
Electronic and Electrical Engineering Department
the University of Sheffield
Sheffield, UK
hfu1@sheffield.ac.uk

Timothy O'Farrell, Senior Member, IEEE
Electronic and Electrical Engineering Department
the University of Sheffield
Sheffield, UK
t.ofarrell@sheffield.ac.uk

***Abstract*—The base station (BS) densification in Internet of Things (IoT) networks provides a viable pathway for enhancing network capacity to meet the ever increasing demand for data. Increasing the number of BSs also increases the energy consumption, which compromises the network energy efficiency (EE). This is important in 3 dimensional (3D) IoT deployments where volume spectral efficiency (VSE) and EE are key performance indicators (KPIs). In such networks, BS sleep modes provide an effective way to constrain both the interference and energy consumption, thereby improving the EE. In this paper, both the VSE and EE of a densified 3D IoT network are investigated when BS and UE counts follow independent 3D Homogeneous Poisson Point Process (HPPP) models and UEs are placed either uniformly or in clusters. The simulation results show that when unloaded BSs are turned off completely, including the backhaul, sufficiently densified 3D IoT networks can be made energy efficient.**

***Index Terms*—Energy Efficiency, Volume Spectral Efficiency, ultra-dense networks, small cell densification, Internet of Things, sleep mode, Spectral Efficiency, 5G Networks, 6G Networks**

I. Introduction

Small cell base station (BS) densification is an effective solution for increasing radio access network (RAN) capacity to cope with the ever increasing user demand for more data [1], [2], [3]. As data becomes more heterogeneous with very diverse quality of service requirements, the IoT network is evolving into an Internet of Everything (IoE) with different types of user equipment (UE) exchanging data with different types of BSs [4], [5]. Improving the capacity of IoT networks through BS densification is expected to meet this growing data demand.

To model the IoT scenario where both the UEs and BSs could be anywhere within a given geographic space [6], [7], the conventional 2 dimensional (2D) planar model employed in most literature, for example, [8], [9], [10], becomes inaccurate. Instead, a 3D model which introduces a third degree of freedom in the vertical direction is more appropriate [11], [12]. Building on the authors' previous work in [13], [14], [15], [16], the contributions of this paper include the use of 3D Homogeneous Point Poisson Process (HPPP) models [17] for determining both BS and UE counts and the use of both clustered and uniform distributions for positioning UEs. Independent 3D HPPP models allow identical BSs and UEs to be distributed randomly within a pre-defined space. In addition, the RAN capacity performance is evaluated using a volume spectral efficiency (VSE) metric for the 3D deployment, whereas energy efficiency performance is evaluated using the RAN energy efficiency (EE) metric.

Despite the potential benefits of improved capacity and EE, BS densification in RANs typically leads to increased network energy consumption due to the larger number of BSs installed in a given geographic area [18], [19]. This eventually compromises the RAN EE since densification increases the RF interference, which reduces capacity, as well as increasing the network energy consumption. Often, the open literature focuses on investigating the capacity enhancement or EE improvement obtained with densification without addressing the underlying increase in network energy consumption [20], [21]. BS sleep modes provide an effective solution to this problem in a densified RAN without needing to change the deployed infrastructure [22]. With BS sleep modes, unloaded BSs without UE associations, or empty cells, may be put into low power sleep modes with reduced RF transmission power and reduced traffic independent operational power. Therefore, BS sleep modes both constrain the RF interference and reduce the energy consumption leading to improved EE.

In this work, the VSE and EE of a densified 3D IoT network is investigated as the BS density is increased with different sleep mode depths and UE densities as parameters. Using a 3D IoT network model with either a uniform or clustered UE distribution, the simulation results show that without any BS sleep modes, the RAN VSE first increases but then decrease with increasing BS density in a pre-defined space, whereas the RAN EE decreases monotonically. However, with BS sleep modes, both the RAN VSE and EE recover providing all the empty cells are turned off completely, including the backhaul. Both observations hold for the different UE distributions and UE densities considered.

The remainder of this paper is organised as follows. Section II introduces the 3D HPPP system model as well as the evaluation metrics used in the study. Section III presents the UE uniform and clustered distributions, the simulation results and a discussion of the results. Finally, section IV provides the conclusions.

ISBN 978-3-903176-49-2

II. System Model

A. Simulation Model

The downlink (DL) traffic of a Long Term Evolution (LTE) IoT RAN is considered in this work. All the BSs in set $\mathcal{B}$ in the RAN are identical with a density of λ_{BS} BS/m^3 according to a 3D HPPP distribution model. A typical-UE is assumed to be at the centre of a cuboid space, with an additional set of virtual-UEs that follows another independent 3D HPPP model with density λ_{VUE} UE/m^3 within the same space. Virtual-UEs are distributed to activate BSs. All the BSs and UEs are assumed to have isotropic antenna. The UE association rule is based on the strongest power received. BSs with the typical-UE or any VUE associations are considered active and fully loaded. In contrast, the remaining BSs are empty and unloaded. The traffic model is full buffer so that UEs are always in demand of data on DL.

The power in dBm received by the typical-UE from its serving BS b_0 on a certain LTE Resource Block (RB) n is given by:

$$\begin{aligned} P_{rx,b_0,n}\ [\text{dBm}] =& P_{tx,b_0,n}\ [\text{dBm}] + G_{BS}\ [\text{dBi}] \\ &+ G_{UE}\ [\text{dBi}] - L_{b_0,n}\ [\text{dB}] \end{aligned} \tag{1}$$

where $P_{tx,b_0,n}$ is the per-RB transmission power from BS b_0; BS and UE antenna gains G_{BS} and G_{UE} between b_0 and the typical-UE, respectively, are both 0 dBi; and $L_{b_0,n}$ is the channel loss of the given RB, including both the large scale pathloss (PL) and shadow fading (SF), as well as the small scale Rayleigh multipath fading (MPF). The transmission power level from an arbitrary BS b depends on the normalised load activity factor α_b, which is unity if b is in an active cell and 0.1 [23] if b is in an empty cell without UE association.

The generic expression for the PL at 3D distance d_{b_0} away from the BS b_0 in dB is given by:

$$PL = \begin{cases} PL_1(d_{b_0})\ [\text{dB}] & d_{b_0} \le d_1 \\ PL_2(d_{b_0})\ [\text{dB}] & d_1 < d_{b_0} \le d_2 \\ PL_3(d_{b_0})\ [\text{dB}] & d_{b_0} > d_2 \end{cases} \tag{2}$$

where d_1 and d_2, which are set to 200 m and 500 m in this work, differentiate the pathloss models, PL_i, $i = 1, 2, 3$, used for the a certain distance range, whose expressions are:

$$PL_i = \begin{cases} \beta_{i,LoS} + \zeta_{i,LoS} \times \log_{10}(d_{b_0})\ [\text{dB}] & \text{if LoS} \\ \beta_{i,NLoS} + \zeta_{i,NLoS} \times \log_{10}(d_{b_0})\ [\text{dB}] & \text{if NLoS} \end{cases} \tag{3}$$

$i = 1, 2, 3$, where both the dimensionless constant β_i and pathloss components ζ_i depend on the signal carrier frequency and transmission environment. Both these constants are differentiated by the LoS and NLoS transmission path conditions. This adopted PL model captures the dependence of signal fading on distance, and is multi-piece probability weighted as suggested in [24], [25] and applied in [8]. Eq. (2) and (3) from the 3GPP documents are designed to cover the terrestrial traffic. They are applied into the 3D model in this work where BSs and UEs are spread over the ground within reasonable cuboid height. The multi-piece LoS probability from [24], [25] is given in (4) at the top of the following page.

Without loss of generality, the SF is modelled as a normal distribution for simplicity with mean μ_{SF} and standard deviation σ_{SF} as suggested in [24] and [25]. The Rayleigh multipath fading is modelled as an independent and identical distribution (iid) random variable [26]. The combined fading effects in dB for a specified range case i, $i = 1, 2, 3$, is given by:

$$\begin{aligned} L_{b_0,n,i} =& \Big(PL_{i,LoS}(d_{b_0}) + SF_{i,LoS}\Big) \times P_{i,LoS}(d_{b_0}) \\ &+ \Big(PL_{i,NLoS}(d_{b_0}) + SF_{i,NLoS}\Big) \\ &\times \big(1 - P_{i,LoS}(d_{b_0})\big) + MPF_n\ [\text{dB}] \end{aligned} \tag{5}$$

The Signal-to-Noise-plus-Interference-Ratio (SINR) experienced by the typical-UE on RB n is then:

$$\gamma_{b_0,n} = \frac{P_{rx,b_0,n}}{\sum_{b\in\mathcal{B},b\neq b_0} P_{rx,b,n} + {\sigma_n}^2}. \tag{6}$$

where $\sum_{b\in\mathcal{B},b\neq b_0} P_{rx,b}$ is the total interference received by the typical-UE, and σ_n is the standard deviation of the noise on the UE side in the DL, including the thermal noise at 293 K and a 4 dB noise figure [26]. Then the throughput of the typical-UE may be calculated using the Shannon capacity formula for an arbitrary Transmission Time Interval (TTI) by:

$$S_{UE} = \frac{12 \times 14 \times \sum_{n=1}^{n_{RB}} \log_2\Big(1 + \gamma_{b_0,n}\Big)}{\delta_t} \tag{7}$$

where 12 is the subcarrier number included in RB n, 14 is the symbol number included in RB n, n_{RB} is the total RB number per TTI, and δ_t is the 1 ms time duration of a TTI. The typical-UE is assumed to occupy all the resource provided by the serving BS b_0. Therefore, all the n_{RB} RBs available in a TTI from the serving BS b_0 are allocated to the typical-UE for all TTIs considered.

B. Evaluation Metrics

This work uses 2 performance metrics to evaluate the capacity and energy efficiency of the 3D HPPP modelled BS densification in the IoT RANs. The capacity metric is RAN VSE in units of bit/s/Hz/m^3, and the energy efficiency metric is the RAN Energy Efficiency in units of bit/J.

The RAN VSE is defined as:

$$VSE_{RAN} = \frac{N_{UE} \times S_{UE}}{B_{b_0} \times V_{RAN}} \tag{8}$$

where N_{UE} is the number of virtual-UEs and the single typical-UE, $N_{UE} \times S_{UE}$ calculates the RAN throughput assuming the typical-UE uses all the resource provided by b_0, B_{b_0} is the total channel bandwidth for signal transmission, and V_{RAN} is the volume in cubic metres of the cuboid space occupied by the RAN, which is calculated by the multiplication of the cuboid length, width, and height. The RAN throughput mapped from the typical-UE throughput provides an upper bound on the throughput, which becomes accurate for highly densified RANs where each active cell serves a single UE.

$$P_{LoS}(d_{b_0}) = \begin{cases} 0.5 - \min\left(0.5, 5 \times \exp\left(\frac{-156}{d_{b_0}}\right)\right) + \min\left(0.5, 5 \times \exp\left(\frac{d_{b_0}}{30}\right)\right) & d_{b_0} > d_2 \\ \min\left(\frac{18}{d_{b_0}}, 1\right) \times \left[1 - \exp\left(\frac{-d_{b_0}}{36}\right)\right] + \exp\left(\frac{-d_{b_0}}{36}\right) & d_1 < d_{b_0} \leq d_2 \\ \min\left(\frac{18}{d_{b_0}}, 1\right) \times \left[1 - \exp\left(\frac{-d_{b_0}}{63}\right)\right] + \exp\left(\frac{-d_{b_0}}{63}\right) & d_{b_0} \leq d_1 \end{cases} \quad (4)$$

The RAN EE is defined as:

$$EE_{RAN} = \frac{M_{RAN}}{E_{RAN}} \quad (9)$$

based on the definition of EE in [27], where M_{RAN} is the total amount of data transmitted in the RAN with units of bit during a certain time period T, and is determined by the product of the total number of UEs and the amount of data sent to the typical-UE as given by:

$$M_{RAN} = N_{UE} \times \sum_{t=0}^{T} M_{UE,t} = N_{UE} \times \sum_{t=0}^{T} (\delta_t \times S_{UE}) \quad (10)$$

The total RAN energy consumption E_{RAN} during the same T time period is given by:

$$E_{RAN} = T \times P_{RAN} = T \times \sum_{b \in \mathcal{B}} P_b(\alpha_b) \quad (11)$$

where

$$P_b(\alpha_b) = P_{RH}(\alpha_b) + P_{OH} \quad (12)$$

is the BS power consumption [28], partly dependent on the normalised load activity factor α_b. An active BS b has α_b=1 [23]; and an empty BS b has α_b=0.1 [23] without sleep mode on or α_b=0 with sleep mode on [1]. The subscript RH stands for radio head and P_{RH} accounts for the traffic dependent part of the BS power consumption [29]. In contrast, P_{OH} calculates the traffic independent part of the BS power consumption including the backhaul, where OH stands for overhead. Based on the expressions in (10) and (11), the RAN EE can be written as:

$$EE_{RAN} = \frac{N_{UE} \times S_{UE}}{P_{RAN}} \quad (13)$$

if both M_{RAN} and E_{RAN} are divided by T. Similarly, the RAN EE mapping the M_{UE} to M_{RAN} becomes accurate for high BS densities, before which RAN EE provides an upper bound on EE.

III. Simulation Results

This section evaluates the VSE and EE performance of a densified IoT RAN with a clustered UE distribution. Within a 100 m × 100 m × 30 m cuboid space, 2 to 1000 BSs are uniformly and randomly scattered. The equivalent BS density is listed in Table I. A total of N_{UE} active UEs are placed in the same space comprising the typical-UE placed at the cuboid centre and $N_{UE} - 1$ virtual-UEs. For the uniform distribution of UEs, the virtual-UEs are randomly uniformly scattered throughout the cuboid space. For the clustered distribution of UEs, one third of the virtual-UEs are randomly uniformly scattered in the cuboid space, while the rest are randomly uniformly scattered in five randomly placed spherical clusters each with 1.5 m radius (i.e., a typical room size). The considered virtual-UE counts and the corresponding densities are given in Table I. The variation of both the BS and virtual-UE heights within the 0 to 30 m range and the fact that BSs could either be below or above the typical UE using this 3D model reflect realistic IoT scenarios with more accuracy than a conventional fixed height 2D model [10]. Other key simulation parameters regarding transmission channel conditions and channel loss are listed in Table I as well. Case 1 to 3 in the table refers to the 3GPP hotspot, urban micro (UMi), and urban macro (UMa) scenarios, respectively [25], [24]. Based on the chosen threshold distances stated in Section II and the cuboid space dimension mentioned above, only case 1, the 3GPP hotspot scenario, is considered in this paper.

TABLE I
Simulation Parameters

Case index i	$i=1$	$i=2$	$i=3$
BS count in RAN	2 - 1000		
BS density λ_{BS} per m^3	0.000007 - 0.003333		
Virtual UE count N_{UE} in RAN	99, 199, 499		
Virtual UE density λ_{VUE} per m^3	0.000330, 0.000663, 0.001663		
UE density λ_{UE} per m^3	0.000333, 0.000667, 0.001667		
Carrier frequency [GHz]	2		
Channel bandwidth [MHz]	20		
RB count per TTI (n_{RB})	100		
BS transmission power ($P_{tx,b}$) [dBm]	21.14		
Pathloss β_{LoS} [dB]	41.1	34.02/4.02	30.8
Pathloss β_{NLoS} [dB]	2.9	30.5	32.9
Pathloss ζ_{LoS}	20.9	22/40	24.2
Pathloss ζ_{NLoS}	42.8	36.7	37.5
Shadow fading μ_{SF} [dB]	0, 0		
Shadow fading $\sigma_{SF,LoS}$ [dB]	10	3	8
Shadow fading $\sigma_{SF,NLoS}$ [dB]	10	4	8
Noise variance σ_n^2 [dBm] per RB	-117.38		

When a BS has UE association, it is active with α being unity, and has all the overhead components on. Based on (12), the power consumption of such an active BS is $P_{RH}(\alpha = 1) + P_{OH,on}$. In contrast, if the BS does not have UE association, it transmits a low power pilot only but has all the overhead components on. The power consumption of such an empty BS is $P_{RH}(\alpha = 0.1) + P_{OH,on}$ and this status is denoted in the results as sm=0. If the sleep mode is on, the empty BS does not transmit the pilot to reduce interference, but can either keep all the overhead components on, or keep only the backhaul (bh) on, or turn all the overhead components including the backhaul off to save energy. The power consumption of an empty BS in sleep mode is thus $P_{RH}(\alpha = 0) + P_{OH,on}$, $P_{RH}(\alpha = 0) + P_{OH,bh}$, and $P_{RH}(\alpha = 0) + P_{OH,off}$, respectively. These increasing sleep mode depths are referred as sm=1, sm=2, and

TABLE II
PARAMETERS FOR BS POWER CONSUMPTION

Item	Value [W]	Item	Value [W]
$P_{RH}(\alpha = 1)$	0.4134	$P_{OH,on}$	9.7059
$P_{RH}(\alpha = 0.1)$	0.1307	$P_{OH,BH}$	5
$P_{RH}(\alpha = 0)$	0	$P_{OH,off}$	0

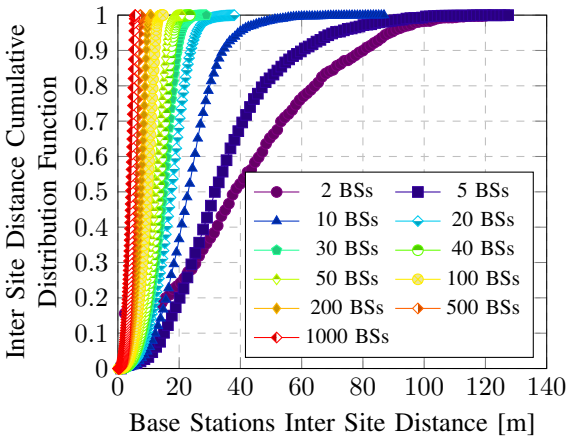

Fig. 1. Cumulative Distribution Function versus ISD for various BS counts

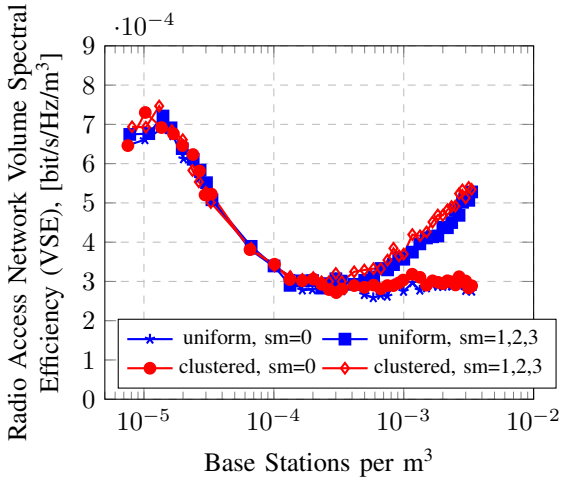

Fig. 2. RAN Volume Spectral Efficiency (VSE) versus BS density for sleep mode on (sm=1,2,3) and off (sm=0) and different UE distributions, 100 UEs

sm=3, respectively. The BSs remain in sleep mode until new UEs enter the coverage area. The parameters are listed in Table II [29].

Fig. 1 plots the Cumulative Distribution Function (CDF) versus BS ISD with the number of BSs as a parameter. Densification adds more BSs into the same space, reducing the ISDs as well as the BS-UE separation. The results show that increasing the number of BSs from 2 to 100 to 1000, the average ISD reduces from 38.66 m to 9.60 m to 4.29 m, respectively. For this ISD range, the BS-UE separations is smaller, hence, both the signal and interference power at the typical-UE from all transmitting BSs are high. Thus the typical-UE is interference limited with interference dominating the capacity performance.

Fig. 2 graphs the IoT RAN Volume Spectral Efficiency versus BS density with both sleep mode status and UE distribution as parameters for a RAN UE count of 100. When sleep mode is off (sm=0), the typical UE briefly experiences a capacity benefit from densification, which increases the UE throughput and thus RAN VSE. With further BS densification, the high interference from both active and empty BSs leads to a decrease in UE throughput and RAN VSE. This tendency is observed for both uniform and clustered UE distributions with the optimum performance turning point around 0.000014 BS/m^3 (4 BSs in the RAN). The RAN VSE then decreases quickly for BS densities up to 0.000066 BS/m^3 (20 BSs in the RAN) when the average distance between UEs and BSs changes rapidly, which is reflected in Fig. 1. With further BS densification, the rate of change in UE-BS separation slows, leading to a decrease in the RAN VSE gradient. However, the uniform UE distribution achieves slightly lower RAN VSE than the clustered distribution. This is because the clustered UEs activate fewer BSs than the uniform case resulting in less RF interference. When sleep mode is on, all of the modes sm=1, 2, and 3 turn off the RF transmission from empty cells, which is more effective at high BS densities. Therefore, with sleep modes the RAN VSE starts to increase at 0.000234 and 0.000334 BS/m^3 (70 and 100 BSs in the RAN) for uniform and clustered UE distributions, respectively. Again, the lower interference due to clustered UEs activating fewer BSs enables slightly higher VSE at high BS densities.

Fig. 3 graphs the IoT RAN Energy Efficiency versus BS density with sleep mode status and UE distributions as parameters for 100 UEs in the RAN. As mentioned, sm=1, 2, and 3 reflect the increasing sleep mode depth that reduces the power consumption of an empty cell. Without sleep mode switched on, all the BSs consume energy all the time. Thus increasing the BS density also increases the RAN energy consumption, which degrades the energy efficiency. This is reflected by the decreasing RAN EE for both types of UE distribution and is related to the decreasing RAN VSE. Again, the clustered UE distribution activates fewer BSs than the uniform case, leading to higher capacity, lower energy consumption, and consequently higher energy efficiency. However, this does not change the overall decreasing EE tendency. Similarly, the reduction in energy consumption from turning off pilot transmission while leaving either the overhead on (sm=1) or just the backhaul on (sm=2) does not affect the decreasing EE tendency, even though capacity is improved. Only when the overhead including backhaul is turned off in empty cells (sm=3), i.e., when empty cells are completely shut down, does EE increase again. This is because the overall energy consumption is prevented from increasing substantially in the high densification region. The turning point occurs at 0.0001 BS/m^3 (300 BSs in the RAN) for both UE distributions, which is slightly higher than the VSE turning point at 0.000066 BS/m^3. Again, the RAN EE is slightly higher when a clustered

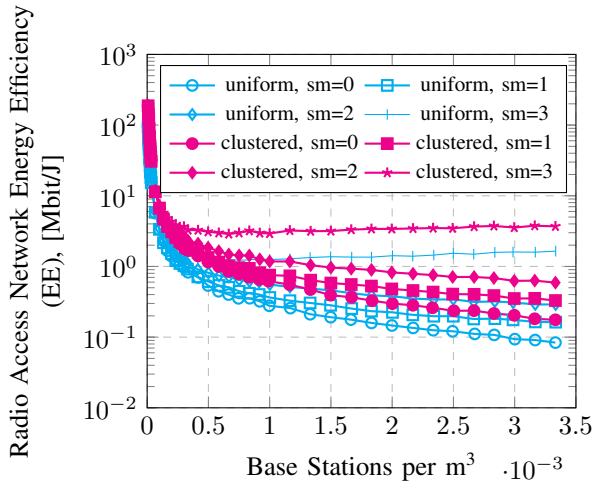

Fig. 3. RAN Energy Efficiency (EE) versus BS density for different UE distributions and empty cell status: sm=0 for sleep mode off , sm=1 for sleep mode on and OH on, sm=2 for sleep mode on and backhaul on, sm=3 for sleep mode on and OH off

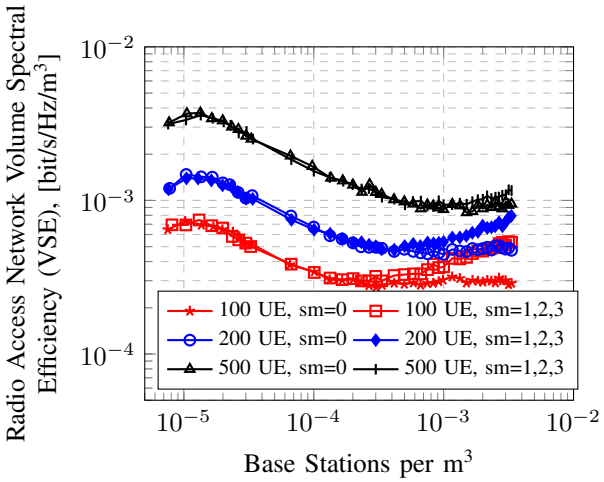

Fig. 4. RAN Volume Spectral Efficiency (VSE) versus BS density for sleep mode on and off and various UE counts, clustered UE distribution

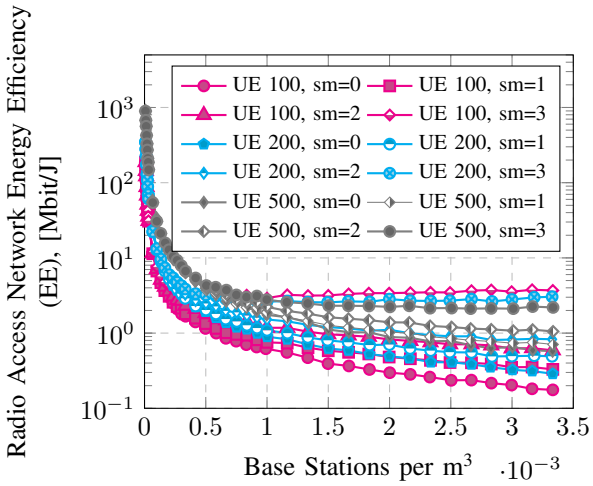

Fig. 5. RAN Energy Efficiency (EE) versus BS density for different UE counts and empty cell status: sm=0 for sleep mode off , sm=1 for sleep mode on and OH on, sm=2 for sleep mode on and backhaul on, sm=3 for sleep mode on and OH off, clustered UE distribution

UE distribution is used due to the lower BS interference.

Fig. 4 graphs the IoT RAN Volume Spectral Efficiency versus BS density with both sleep mode status and UE count as parameters. Though higher UE densities result in higher VSEs, the change in UE density does not affect the RAN VSE vs. BS density trend. First, the VSE increases due to higher received signal power but then decreases due to higher received interference power. When sleep mode is off (sm=0) the VSE levels off, whereas with sleep mode on (sm=1,2,3) it starts to increase again. However, the amount of this increase and associated turning point depend on the UE density. The larger the UE density the smaller the capacity increase and the greater the BS density turning point as more BSs are activated, which increases interference. Though there are no available EE results for a 3D model that the authors are aware of, the work in [8] has the similar capacity improvement performance against the BS densification using a 2D model with the sleep mode between different UE densities. However, the results in [8] do not capture the quick capacity degradation due to severe interference.

Fig. 5 graphs the IoT RAN Energy Efficiency versus BS density with sleep mode status and UE count as parameters. The RAN EE curves for the same UE density behave similarly as the BS density increases. Again, adding more UEs to the same space activates more BSs for a certain BS density, which increases the RAN energy consumption. This effect is the most prominent for sm=3 where the power consumption of active and empty BSs differs the most. The improvement in capacity with UE density shown in Fig. 4 off sets this energy consumption increase to some extent. As a result, the RAN EE increases with UE count from 100 to 500 for sm=0, 1, and 2, albeit with diminishing steps. In contrast, for sm=3 the RAN EE first improves with increasing UE count for small BS densities up to 0.000998 BS/m^3 (300 BSs in the RAN) and then decreases with increasing UE count. The reduction in EE with increasing UE count for sm=3, corresponds to the region in Fig. 4 when the capacity turning points shift to higher BS densities at higher UE counts. The work in [1] has a similar EE improvement against the BS density using a 2D model when sleep mode is enabled. However, the EE degradation at low BS densities is not captured in [1].

IV. Conclusions

The BS densification in IoT RANs is evaluated in this work using the metrics of RAN volume spectral efficiency (VSE) and RAN energy efficiency (EE). The application of sleep mode with different depths has also been investigated. Both BS and UE counts follow independent 3D HPPP distributions, which provide three degrees of spatial freedom compared with conventional 2D models. Also, performance for uniform

and clustered UE distributions is investigated. The simulation results show that without any sleep mode, the BS densification in IoT networks would degrade RAN VSE due to interference, and also degrade the RAN EE due to both VSE decrease and energy consumption increase. In contrast, placing empty cells into sleep mode constrains the interference, which improves the RAN VSE when the IoT network is sufficiently dense. However, the RAN EE only improves at high BS densities when all the empty cells are turned off completely, including the backhaul. These observation hold for both uniform and clustered UE distributions. For future work, mathematical analysis of SINR and UE/RAN throughput will be carried out under the 3D HPPP model and extended to heterogeneous network deployments.

REFERENCES

[1] D. López-Pérez, M. Ding, H. Claussen, and A.H. Jafari, "Towards 1 Gbps/UE in cellular systems: understanding ultra-dense small cell deployments," in *IEEE Commun. Surv. Tutor.*, vol. 17, issue 4, Jun. 2015, pp. 2078-2101

[2] J. Hoydis, M. Kobayashi, and M. Debbah, "Green small-cell networks," in *IEEE Veh. Technol. Mag.*, vol. 6, issue 1, Mar. 2011, pp. 37-43

[3] J. G. Andrews, S. Buzzi, W. Choi, S. V. Hanly, A. Lozano, A. C. K. Soong, and J.Z. Charlie Zhang, "What will 5G be?" in *IEEE J-SAC*, vol. 32, issue 6, Jun. 2014, pp. 1065-1082

[4] J.S. Liu, C-H R. Lin, Y.C Hu, and P. K. Donta, "Joint beamforming, power allocation, and splitting control for SWIPT-enabled IoT networks with deep reinforcement learning and game theory," in *Sensors 2022*, no. 6: 2328, Mar. 2022, https://doi.org/10.3390/s22062328

[5] F. Al-Turjman, E. Ever, and H. Zahmatkesh, "Small cells in the forthcoming 5G/IoT: traffic modelling and deployment overview," in *IEEE Commun. Surv. Tutor.*, vol. 21, issue 1, Firstquarter 2019, pp. 28-65

[6] E. Sisinni, A. Saifullah, S. Han, U. Jennehag, and M. Gidlund, "Industrial Internet of Things: challenges, opportunities, and directions," in *IEEE Trans. Industr. Inform.*, vol. 14, issue 11, Nov. 2018, pp. 4724-4734

[7] K. K. Wong and T. O'Farrell, "Coverage of 802.11g WLANs in the presence of Bluetooth interference," in *14th IEEE Proceedings on Personal, Indoor and Mobile Radio Communications (PIMRC)*, 2003, vol.3, pp. 2027-2031

[8] M. Ding, D. López-Pérez, Y. Chen, G. Mao, Z. Lin, and A. Y. Zomaya, "Ultra-dense networks: a holistic analysis of multi-piece path loss, antenna heights, finite users and BS idle modes," in *IEEE Trans. Mob. Comput.*, vol. 20, no. 4, 1 April 2021, pp. 1702-1713

[9] C. Ma, M. Ding, D. López-Pérez, Z. Lin, J. Li, and G. Mao, "Performance analysis of the idle mode capability in a dense heterogeneous cellular network," in *IEEE Trans. Commun.*, vol. 66, issue 9, Sept. 2018, pp. 3959-3973

[10] M. Ding, D. López-Pérez, G. Mao, and Z. Lin, "Performance impact of idle mode capability on dense small cell networks," in *IEEE Trans. Veh. Technol.*, vol. 66, issue 11, Nov. 2017, pp. 10446-10460

[11] Cordis, "Beyond 5G: 3D network modelling for THz-based ultra-fast small cells", in *5G-ACE, Horizon 2020*, Accessed on: 21 Mar 2022, [online]. Available: https://cordis.europa.eu/project/id/839573/reporting/de

[12] I. Yaqoob et al., "Internet of Things architecture: recent advances, taxonomy, requirements, and open challenges," in *IEEE Wirel. Commun.*, vol. 24, issue 3, June 2017, pp. 10-16

[13] B. Badic, T. O'Farrell, P. Loskot and J. He, "Energy Efficient Radio Access Architectures for Green Radio: Large versus Small Cell Size Deployment," in *2009 IEEE 70th Vehicular Technology Conference Fall*, 2009, pp. 1-5, doi: 10.1109/VETECF.2009.5379035.

[14] I. Martin et al., "A High-Resolution Sensor Network for Monitoring Glacier Dynamics," in *IEEE Sensors Journal*, vol. 14, no. 11, pp. 3926-3931, Nov. 2014, doi: 10.1109/JSEN.2014.2348534.

[15] W. Guo, S. Wang, Y. Wu, J. Rigelsford, X. Chu and T. O'Farrell, "Spectral- and energy-efficient antenna tilting in a HetNet using reinforcement learning," in *2013 IEEE Wireless Communications and Networking Conference (WCNC)*, 2013, pp. 767-772, doi: 10.1109/WCNC.2013.6554660.

[16] Weisi Guo, C. Turyagyenda, H. Hamdoun, Siyi Wang, P. Loskot and T. O'Farrell, "Towards a low energy LTE cellular network: Architectures," in *2011 19th European Signal Processing Conference*, 2011, pp. 879-883.

[17] N. Cressie, "4 - Models for spatial process," in *Methods in Experimental Physics*, vol. 28, J.L. Stanford, S.B. Vardeman, Ed. Academic Press, 1994, pp. 93-124

[18] O. Alamu, A. Gbenga-Ilori, M. Adelabu, A. Imoize, and O. Ladipo, "Energy efficiency techniques in ultra-dense wireless heterogeneous networks: An overview and outlook," in *Engineering Science and Technology, an International Journal*, vol. 23, issue 6, May 2020, pp. 1308-1326

[19] H. Shokri-Ghadikolaei, C. Fischione, P. Popovski, and M. Zorzi, "Design aspects of short-range millimeter-wave networks: A MAC layer perspective," in *IEEE Network*, vol. 30, no. 3, May-June 2016, pp. 88-96

[20] Y. Li, P. Fan, A. Leukhin, and L. Liu, "On the spectral and energy efficiency of full-duplex small-cell wireless systems with massive MIMO," in *IEEE Trans. Veh. Technol.* vol. 66, issue 3, Mar. 2017, pp. 2339-2353

[21] I. AlQerm, and B. Shihada, "Energy-efficient power allocation in multi-tier 5G networks using enhanced online learning," in *IEEE Trans. Veh. Technol.*, vol. 66, issue 12, Dec. 2017, pp. 11086-11097

[22] J.J. Wu, Y.J. Zhang, M. Zukerman, and K.-N. Yung, "Energy-efficient base-stations sleep-mode techniques in green cellular networks: a survey," in *IEEE Commun. Surv. Tutor.*, vol. 17, issue 2, Secondquarter 2015, pp. 803-826

[23] T. O'Farrell, and S.C. Fletcher, "Green communication concepts, energy metrics and throughput efficiency for wireless systems," in *Green Communications: Principles, Concepts and Practice* 1st ed, K. Samdanis, P. Rost, A. Maeder, M. Meo, and C. Verikoukis Eds. John Wileys & Sons. Ltd, 2015, Chap 2, pp. 19-42

[24] 3rd Generation Partnership Project, "TR 36.814: 3rd generation partnership project; technical specification group radio access network; evolved universal terrestrial radio access (E-UTRA); further advancements for E-UTRA physical layer aspects (release 9)", Mar. 2017, V9.2.0

[25] 3rd Generation Partnership Project, "TR 36.828: 3rd generation partnership project; technical specification group radio access network; evolved universal terrestrial radio access (E-UTRA); further enhancements to LTE Time Division Duplex (TDD) for Downlink-Uplink (DL-UL) interference management and traffic adaptation (release 11)", V11.0.0, Jun. 2012

[26] H. Fu, and T. O'Farrell, "An Energy Efficiency evaluation framework for Radio Access Networks," in *2018 International Conference on Information and Communication Technology Convergence (ICTC)*, 2018, pp. 577-580

[27] 3rd Generation Partnership Project, "Environmental engineering (EE); assessment of mobile network energy efficiency", ETSI ES 203 228, Jan. 2015, V1.0.0

[28] A. Arbi, and T. O'Farrell, "Energy efficiency in 5G access networks: Small cell densification and high order sectorisation," in *2015 IEEE International Conference on Communication Workshop (ICCW)*, 2015, pp. 2806-2811

[29] A. Arbi, T. O'Farrell, F.-C. Zheng, and S.C. Fletcher, "Toward green evolution of cellular networks by high order sectorisation and small cell densification," in *Interference Mitigation and Energy Management in 5G Heterogeneous Cellular Networks*, Jan. 2017